work and could not reproduce the relative heights in the rotational TOF peaks experimentally observed at $E_{col} = 1.28$ eV.

Our data demonstrate that the theoretical results, especially the accurate QM ones, on the reactive scattering of H + D_2 ($v = 0, j = 0$) are essentially correct even at the high level of resolution now obtained. Moreover, the QCT approach seems to provide a very good description of scattering angular distributions to the level of vibrational resolution of the products but leads to some differences when individual rotational states can be resolved. No refinements in the ab initio LSTH PES (*16*) seem necessary, at least for the energies of the experiment. This work shows that the present experimental results at $E_{col} = 1.28$ eV ($E = 1.47$ eV) and under the specified conditions can be explained without explicit consideration of the GP effect.

REFERENCES AND NOTES

1. H. Buchenau, J. P. Toennies, J. Arnold, J. Wolfrum, *Ber. Bunsenges. Phys. Chem.* **94**, 1231 (1990).
2. W. H. Miller, *Annu. Rev. Phys. Chem.* **41**, 245 (1990); J. Z. H. Zhang and W. H. Miller, *Chem. Phys. Lett.* **153**, 465 (1988); *ibid.* **159**, 130 (1989); *J. Chem. Phys.* **91**, 1528 (1989).
3. M. Mladenovic *et al.*, *J. Phys. Chem.* **92**, 7035 (1988); M. Zhao, D. G. Truhlar, N. C. Blais, D. W. Schwenke, D. J. Kouri, *ibid.* **94**, 6696 (1990); D. G. Truhlar, D. W. Schwenke, D. J. Kouri, *ibid.*, p. 7346.
4. R. T. Pack and G. A. Parker, *J. Chem. Phys.* **87**, 3888 (1987); *ibid.* **90**, 3511 (1989); J. D. Kress, Z. Bacic, G. A. Parker, R. T. Pack, *Chem. Phys. Lett.* **157**, 585 (1989); *ibid.* **170**, 306 (1990).
5. D. E. Manolopoulos and R. E. Wyatt, *Chem. Phys. Lett.* **152**, 23 (1988); D. E. Manolopoulos, M. J. D'Mello, R. E. Wyatt, *J. Chem. Phys.* **91**, 6096 (1989).
6. D. E. Manolopoulos, M. J. D'Mello, R. E. Wyatt, *J. Chem. Phys.* **93**, 403 (1990); M. J. D'Mello, D. E. Manolopoulos, R. E. Wyatt, *Chem. Phys. Lett.* **168**, 113 (1990); D. E. Manolopoulos, M. J. D'Mello, R. E. Wyatt, R. B. Walker, *ibid.* **169**, 482 (1990); M. J. D'Mello, D. E. Manolopoulos, R. E. Wyatt, *J. Chem. Phys.* **94**, 5985 (1991).
7. Y. M. Wu, B. Lepetit, A. Kuppermann, *Chem. Phys. Lett.* **186**, 319 (1991); Y. M. Wu and A. Kuppermann, *ibid.* **201**, 178 (1993); A. Kuppermann and Y. M. Wu, *ibid.* **205**, 577 (1993); *ibid.* **213**, 636 (1993).
8. J. C. Nieh and J. J. Valentini, *Phys. Rev. Lett.* **60**, 519 (1988); D. L. Phillips, H. B. Levene, J. J. Valentini, *J. Chem. Phys.* **90**, 1600 (1989).
9. D. A. V. Kliner, D. E. Adelman, R. N. Zare, *J. Chem. Phys.* **94**, 1069 (1991).
10. R. E. Continetti, J. Z. H. Zhang, W. H. Miller, *ibid.* **93**, 5356 (1990); W. H. Miller and J. Z. H. Zhang, *J. Phys. Chem.* **95**, 7767 (1991).
11. F. J. Aoiz, V. J. Herrero, V. Sáez Rábanos, *J. Chem. Phys.* **97**, 7423 (1992).
12. D. A. V. Kliner, D. E. Adelman, R. N. Zare, *ibid.* **95**, 1648 (1991).
13. D. E. Adelman, N. E. Shafer, D. A. V. Kliner, R. N. Zare, *ibid.* **97**, 7323 (1992).
14. D. Neuhauser *et al.*, *Science* **257**, 519 (1992).
15. N. C. Blais, M. Zhao, D. G. Truhlar, D. W. Schwenke, D. J. Kouri, *Chem. Phys. Lett.* **166**, 368 (1990); *ibid.* **188**, 368 (1992); S. L. Mielke, R. S. Friedman, D. G. Truhlar, D. W. Schwenke, D. J. Kouri, *ibid.*, p. 359; W. J. Keogh *et al.*, *ibid.* **195**, 144 (1992).
16. P. Siegbahn and B. Liu, *J. Chem. Phys.* **68**, 2457 (1978); D. G. Truhlar and C. J. Horowitz, *ibid.*, p. 2466; *ibid.* **71**, 1514 (1979).
17. A. J. C. Varandas, F. B. Brown, C. A. Mead, D. G. Truhlar, B. C. Garrett, *ibid.* **86**, 6258 (1987); A. I. Boothroyd, W. J. Keogh, P. G. Martin, M. R. Peterson, *ibid.* **95**, 4343 (1991).
18. F. J. Aoiz, H. K. Buchenau, V. J. Herrero, V. Sáez Rábanos, *ibid.* **100**, 2789 (1994).
19. R. E. Continetti, B. A. Balko, Y. T. Lee, *ibid.* **93**, 5719 (1990).
20. T. N. Kitsopoulos, M. A. Buntine, D. P. Baldwin, R. N. Zare, D. W. Chandler, *Science* **260**, 1605 (1993).
21. S. L. Mielke, D. G. Truhlar, D. W. Schwenke, *J. Phys. Chem.* **98**, 1053 (1994).
22. F. J. Aoiz *et al.*, *J. Chem. Phys.* **101**, 5781 (1994).
23. F. J. Aoiz, V. J. Herrero, O. Puentedura, V. Sáez Rábanos, *Chem. Phys. Lett.* **198**, 321 (1992).
24. M. J. D'Mello, D. E. Manolopoulos, R. E. Wyatt, *Science* **263**, 102 (1994).
25. Y. M. Wu and A. Kuppermann, *Chem. Phys. Lett.* **235**, 105 (1995).
26. L. Schnieder, K. Seekamp-Rahn, F. Liedecker H. Steuwe, K. H. Welge, *Faraday Disc. Chem. Soc.* **91**, 259 (1991).
27. L. Schnieder, W. Meier, K. H. Welge, M. N. R. Ashfold, C. M. Western, *J. Chem. Phys.* **92**, 7027 (1990).
28. N. C. Blais and D. G. Truhlar, *Chem. Phys. Lett.* **102**, 120 (1983); *J. Chem. Phys.* **83**, 2201 (1985).
29. K.-D. Rinnen, D. A. Kliner, R. N. Zare, *J. Chem. Phys.* **91**, 7514 (1989).

30. The experimental part of this project was financed by the German Science Foundation under grants WE 386/19 and SCHN 435/3 and by the Deutscher Akademischer Austauschdienst (Acciones Integradas) 322-Al-e-dr. The Spanish contribution was financed by the Direccion General de Investigacion Cientifica Tecnologica of Spain under grant PB92-0219-C03 and the German-Spanish Scientific Exchange Program "Acciones Integradas" under grants HA-074, HA-113, and HA-135. Research at the University of Texas was supported by the Robert Welch Foundation and the National Science Foundation.

7 March 1995; accepted 3 May 1995

Climate Records Covering the Last Deglaciation

Todd Sowers* and Michael Bender

The oxygen-18/oxygen-16 ratio of molecular oxygen trapped in ice cores provides a time-stratigraphic marker for transferring the absolute chronology for the Greenland Ice Sheet Project (GISP) II ice core to the Vostok and Byrd ice cores in Antarctica. Comparison of the climate records from these cores suggests that, near the beginning of the last deglaciation, warming in Antarctica began approximately 3000 years before the onset of the warm Bølling period in Greenland. Atmospheric carbon dioxide and methane concentrations began to rise 2000 to 3000 years before the warming began in Greenland and must have contributed to deglaciation and warming of temperate and boreal regions in the Northern Hemisphere.

During the late Pleistocene, Earth's climate fluctuated between glacial and interglacial conditions with a period of ~100,000 years. Although changes in Earth's orbit clearly pace climate change, the rapid destruction of the continental ice sheets at the end of a glacial period is not solely the result of simple orbital forcing on the mass balance of the ice sheets. Other factors, such as changes in meridional heat transport by oceans and atmosphere, eustatic sea level rise, changing albedo, and increases in the greenhouse gas concentration, are likely contributors (*1*).

One requirement for understanding the dynamics of a glacial termination is to delineate the sequence of events that characterize it. Here we focus on two elements of the most recent glacial termination: surface temperature records from Greenland and Antarctica and changes in the concentration of greenhouse gases in the atmosphere. We utilize records of the $\delta^{18}O$ of atmospheric O_2 from three ice cores as time stratigraphic markers to transfer the GISP II (central Greenland) varve chronology (*2, 3*) to the Byrd (West Antarctic) and Vostok (East Antarctic) ice cores. We then compare various ice core climate records with each other as well as with marine and terrestrial climate records and summarize the sequence of events during the last glacial termination.

Records of variations in the $\delta^{18}O$ of atmospheric O_2 with time are based on analyses of trapped gases in several ice cores (*4, 5*) (Fig. 1A). One can compute $\delta^{18}O_{atm}$ from the measured $\delta^{18}O$ of trapped O_2 after correcting for gravitational fractionation using the $\delta^{15}N$ of trapped N_2 (*6–8*). The general nature of the $\delta^{18}O_{atm}$ record from the GISP II, Byrd, and Vostok ice cores is similar: low values throughout the Holocene with a minimum at about 10,000 years ago (10 ka); maximum glacial values that are up to 1.3 per mil higher than at present; and intermediate values during marine isotope stage 3. The major factor influencing the $\delta^{18}O$ of atmospheric O_2 during the past 135,000 years was variability in the $\delta^{18}O$ of seawater resulting from variations in the size of the continental ice sheets (*5*). Secondary factors include variable isotope fractionation associated with respiration, evapotranspiration, and the global hydrologic cycle (*9*). At any one time, $\delta^{18}O_{atm}$ is constant throughout the atmosphere because the time for turnover of atmospheric O_2 [~1200 years (*9*)] is long relative to the interhemispheric

Graduate School of Oceanography, University of Rhode Island, Narragansett, RI 02882, USA.

*Present address: Lamont-Doherty Earth Observatory, Palisades, NY 10964, USA.

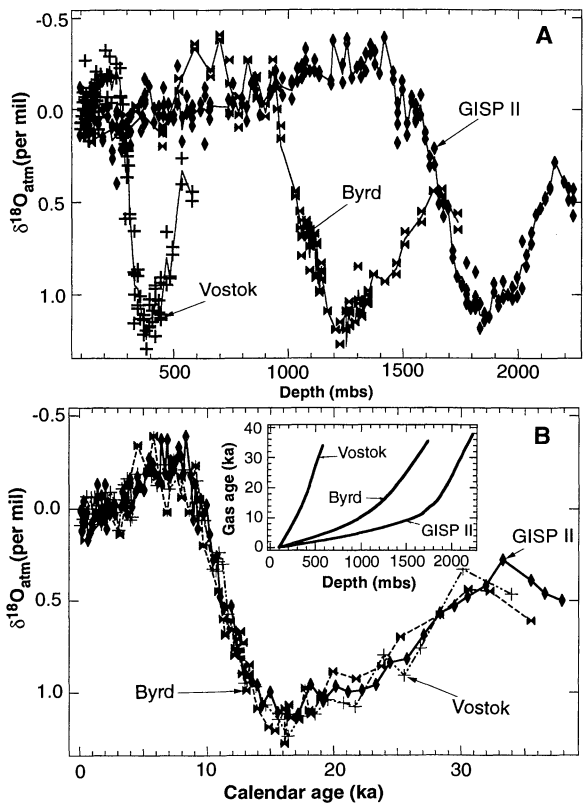

Fig. 1. Records of the $^{18}O/^{16}O$ of paleoatmospheric O_2 as recorded in three ice cores: (**A**) $\delta^{18}O_{atm}$ records from the GISP II (Summit, Greenland), Byrd (West Antarctica), and Vostok (East Antarctica) ice cores plotted as a function of depth. Individual $\delta^{18}O_{atm}$ values (per mil with respect to the present) are plotted along with a line drawn through the mean value. The magnitude of the $\delta^{18}O_{atm}$ variations associated with the glacial-interglacial transition are almost identical (1.4 per mil). The cores are offset from one another because of the different rates of snow accumulation at the three sites. The Byrd and Vostok cores contain longer $\delta^{18}O_{atm}$ records than covered in the first 2250 m of the GISP II core because age in these two cores increases with depth faster than at GISP II. (**B**) The $\delta^{18}O_{atm}$ records (per mil with respect to the present) from the three ice cores as a function of calendar age. The GISP II chronology is based on annual layer counting throughout the top 2250 m (*2, 3*). We constructed the Byrd and Vostok age models by correlating the $\delta^{18}O_{atm}$ records into the GISP II record versus calendar age. The resulting mapping function for the Byrd and Vostok cores is shown in the inset along with the gas age–depth profile for GISP II. The Vostok and Byrd mapping functions each have three coefficients yielding r^2 values of 0.98 and 0.96, respectively. All $\delta^{18}O_{atm}$ data sets are available upon request.

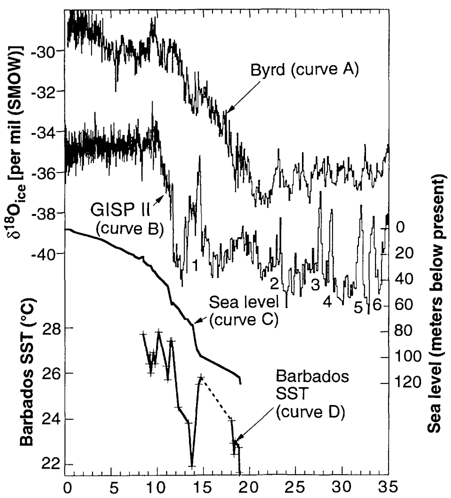

Fig. 2. Climate records spanning the last glacial termination. Isotopic temperature data for Greenland and Antarctica are shown in the top two curves: curve A, the Byrd $\delta^{18}O_{ice}$ record (*56*) and curve B, the GISP II $\delta^{18}O_{ice}$ record (2-m average) from (*57*); SMOW, standard mean ocean water. Curve C plots eustatic sea levels deduced from the Barbados coral record between 19 and 9 ka (*27*), combined with ^{14}C-dated shell material between 9 and 0 ka (*58*). Curve D shows the Barbados SSTs based on the Sr/Ca ratios of the *Acropora palmata* corals (*28*). Interstadial events are numbered.

mixing time (~1 year). We can therefore use $\delta^{18}O_{atm}$ records from different ice cores as time-stratigraphic markers for correlation.

As an absolute reference we used the GISP II time scale (Fig. 1B), which, to a depth of 2250 m, is based on counting annual layers and has an absolute uncertainty of ±3% (*2, 3*). Because air is trapped below the surface of the ice sheet, the bubbles are younger than the surrounding ice. We estimated differences between the ice and gas ages (Δage) in (*4*). Resulting Δage values are 240 ± 50 years for the last 10,000 years and increase to 630 ± 100 years during the last glacial maximum (LGM). We calculated a gas age–depth relation for GISP II by subtracting the Δage estimates from the ice age at each depth down to 2250 m below the surface (mbs).

We constructed gas age models for the Byrd and Vostok cores by correlating their $\delta^{18}O_{atm}$-depth records into the GISP II record of $\delta^{18}O_{atm}$ versus gas age, using an inverse correlation method (*11*). From a comparison of the three $\delta^{18}O_{atm}$ records, it appears as though the time scales for the three cores are consistent with one another throughout the last 35,000 years. This technique is especially well suited to correlating deep ice cores retrieved near the center of the ice sheets where ice flow effects have not disturbed the stratigraphy to any measurable degree (*12*). The correlation provides an accurate means of transferring the GISP II time scale to other ice cores when $\delta^{18}O_{atm}$ changes rapidly over time. The best period for performing the $\delta^{18}O_{atm}$ correlation is between 15 and 8 ka when $\delta^{18}O_{atm}$ decreased by 1.5 per mil. During this interval, we estimate an age error of about ±600 years. Over the last 8000 years as well as between 22 and 30 ka, we can only correlate the two $\delta^{18}O_{atm}$ records to ±1500 years because of the slowly varying $\delta^{18}O_{atm}$ values.

Between 16 and 22 ka, $\delta^{18}O_{atm}$ varied by less than ±0.1 per mil. Thus, during this period, we are unable to provide well-constrained time scales for other ice cores using $\delta^{18}O_{atm}$. However, ages at the top and base of this interval are constrained to about ±600 and ±1500 years, respectively, and limit uncertainties within this interval to less than ±2000 years (much less near the younger end of the interval). Vostok ages between 28 and 33 ka are based on only two $\delta^{18}O_{atm}$ analyses and therefore are highly uncertain.

The isotopic compositions of O and H in ice (denoted $\delta^{18}O_{ice}$ and δD_{ice}, respectively) are related to the condensation temperature over the deposition site (*13–15*). There are, however, other factors [for example, changing source areas and storm tracks (*16*)] that can have a dramatic influence on the isotopic composition of the precipitation. Therefore, the record of $\delta^{18}O_{ice}$ versus time for each ice core must be considered a record of local temperature variation. Fortunately, deep ice cores retrieved from different geographic regions of Greenland and Antarctica show very similar continent-wide $\delta^{18}O_{ice}$ records, suggesting that the major features of these records reflect temperature changes over much of Greenland and Antarctica (*17, 18*).

The two $\delta^{18}O_{ice}$ records from the GISP II and GRIP ice cores from Summit, Greenland, are essentially identical over the last 35 ka (*17*). The shifts in $\delta^{18}O_{ice}$ (5 per mil) between 27 and 35 ka at GISP II (interstadial events 4 to 8) are thought to be related to large-scale shifts in the atmospheric circulation dynamics, which may have been induced by changes in thermohaline circulation in the North Atlantic (*19–21*) (Fig. 2). A $\delta^{18}O_{ice}$ increase, which Johnsen *et al.* (*22*) interpreted as the start of the glacial termination at GRIP–GISP II, began at 24 ka with a moderate (2 per mil) increase followed by a 1 per mil decrease to almost full glacial values near 16 ka. The Bølling interstadial in Greenland began abruptly at 14.7 ka. It was the first instance during the termination in which Greenland temperatures rose above the highest glacial values.

We consider this event to be the first clear indication in the GRIP–GISP II isotopic temperature records that climate over Greenland had shifted out of its glacial mode. The climate shifts reflected in the GISP II $\delta^{18}O_{ice}$ record have been observed in all Greenland ice cores (*17*), in North Atlantic deep-sea sediments (as changes in the abundance of temperature-sensitive planktonic foraminifera) (*20, 21*), and in central Europe (*23*). Thus, the $\delta^{18}O_{ice}$ record from Greenland reflects climate change on a regional or larger scale.

The magnitude of the glacial-interglacial isotopic temperature shifts at Byrd and Vostok, 7° to 10°C, are comparable to those in Greenland (*24*). On the other hand, the timing of the Antarctic warming differs from that in Greenland during the last 35,000 years. The warm interstadial events between 23 and 33 ka in the GISP II record [numbered 2 to 6 (*17*)] are either absent or small in the Byrd record. In Antarctica, the initial isotopic temperature increase associated with Termination 1 began at about 20 ka and continued at a rate of 0.8 per mil per 1000 years until about 11 ka. The first time that the Byrd $\delta^{18}O_{ice}$ values rose above the highest glacial value was at 18 ka. This event preceded the corresponding event recorded in the GISP II core by 3300 years.

The magnitude of the warming observed over the Antarctic continent is similar to the 7° to 10°C increase in sea-surface temperatures (SST) in the Southern Ocean during the last termination (*25, 26*). The start of the SST increase in the Southern Ocean occurred at about 17 ka (*25, 26*), implying that the Southern Ocean SST increase was roughly coincident with the largest part of the temperature increase over the Antarctic continent.

The initial Antarctic temperature increase is also in phase with an increase in eustatic sea level and tropical SSTs as reflected by the Barbados coral record (Fig. 2) (*27, 28*). Moreover, recent evidence of snowline depression along the cordillera of North and South America (*29*) and reduced continental temperatures (*30*) during the last glacial period suggest lower (>5°C) temperatures on a global scale during the last glacial period. Taken at face value, most of these continental records from North America and Europe show temperature increases beginning at about 17 ka (calendar age) (*30*). On the basis of the GISP II $\delta^{18}O_{ice}$ record in Fig. 2, Greenland was, if anything, cooling between 18 ka and 15 ka; this result suggests that the North Atlantic was not responding to the warming in the Southern Hemisphere and tropical regions. In fact, the abrupt warming that initiated the Bølling epoch in the far North Atlantic region occurred at 14.7 ka, 2000 to 4000 years after the initial warming exhibited in most records south of 45°N.

One possible explanation for this apparent lack of synchroneity between the North Atlantic and elsewhere is that a stationary polar front located at 45°N in the North Atlantic effectively insulated areas to the north from the global warming. Data from planktonic foraminifera in North Atlantic deep-sea cores indicate that the polar front did not migrate northward until just before the onset of the Bølling period (14.7 ka) (*31–33*). Keigwin *et al.* (*31*) proposed that, as the Laurentide ice sheet began to retreat, the atmospheric circulation patterns moved northward, thereby allowing the polar front to migrate north toward its present-day position. The Barbados coral record indicates that the most rapid ice sheet deflation occurred during the melt water pulses (MWP) centered at 14.5 and 11.5 ka (calendar age, Fig. 3) (*27, 34*). The migration of the polar front also appears to be synchronous with renewed formation of lower North Atlantic deep water (NADW) as indicated by the increase in benthic $\delta^{13}C$ values in the deep North Atlantic [V23-81 (*35*)] and Southern oceans [RC11-83 (*36*)] and a decrease in the Cd/Ca ratios exhibited in the Bermuda Rise cores (*31*).

Between 12.5 and 14 ka, a small oscillation toward colder conditions is evident in the Byrd isotope temperature record. A similar oscillation occurs in all deglacial isotope temperature records from Antarctica (*24, 37*). The magnitude of the cooling over Antarctica is much smaller than that of the Younger Dryas (Y-D) event recorded in the Greenland ice cores. The $\delta^{18}O_{ice}$ "shoulder" at Byrd ends at 12.5 ka, which is nearly 1000 years earlier than the end of the Y-D event in Greenland. The uncertainty in the difference between the ice age and the gas age throughout this period is ±100 years (*10*) and cannot be invoked as an artifactual cause of this difference in timing. Thus, we believe that the Antarctic oscillation occurred before the Y-D event in Greenland. Given the magnitude and timing of the cold events over Greenland and Antarctica, it is not clear how they may have been related to one another.

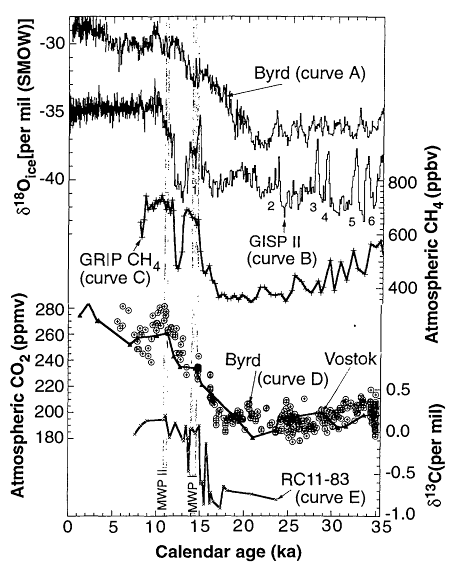

Fig. 3. Antarctic (curve A) and Greenland (curve B) isotope temperature records as in Fig. 2. Curve C plots the atmospheric CH_4 record from (*41*) on the GISP II time scale showing rapid CH_4 oscillations during the interstadial and Y-D events. Curve D plots the Byrd CO_2 record (circled pluses) from (*38, 46*) and the Vostok CO_2 record (solid line) (*59*) on the correlated time scale. Curve E shows the benthic foraminiferal $\delta^{13}C$ record from South Atlantic core RC11-83 (41°36′S, 94°48′E, 4718 m) (*36*). The age model for the $\delta^{13}C$ record is based on atomic mass spectroscopy ^{14}C dates that were converted to calendar ages by means of the CALIB 3.0 program (*60*).

The CO_2 partial pressure records (P_{CO_2}) from Byrd and Vostok show the well-known increase in atmospheric P_{CO_2} from 190 to 200 parts per million by volume (ppmv) during glacial times to 275 ppmv in the early Holocene (Fig. 3). The P_{CO_2} increase began at 17 ka and continued at a rate of 12 ppm per 10^3 years throughout the transition. The Byrd record suggests that there may have been a brief episode, near 14 ka, when the rate of P_{CO_2} increase was reduced.

As noted by Staffelbach *et al.* (*38*), the Byrd CO_2 values are generally more stable than the Greenland values over the last 50,000 years. One puzzling result from the CO_2 analyses on the Dye 3 core (southern Greenland) is the rapid CO_2 fluctuations (>50 ppm), which were in phase with the $\delta^{18}O_{ice}$ variations between interstadial events 3 and 8 (1860 to 1890 mbs) (*39*). If the Dye 3 CO_2 record accurately reflects the composition of the glacial atmosphere, we would expect to see such fluctuations in all ice cores. Close inspection of Fig. 3 shows that the 50-ppm variations are not found in either Antarctic CO_2 record between interstadial events 3 and 7 (27 to 35 ka). There is little to no variation during interstadial events 4 to 6, which were sampled in detail for CO_2 in the Dye 3 record. These results support the suspicion that the glacial CO_2 record from Dye 3 has been compromised, possibly as a result of the extremely high dust concentrations in Greenland during the last glacial period (*40*).

Atmospheric CH_4 concentrations (Fig. 3) measured in the GRIP ice core covaried with temperature during Dansgaard-Oeschger events between 30 and 40 ka, began to rise from full glacial values at 17 ka, and dropped sharply during the Y-D (*41*). These fluctuations probably involve changes in the rates of CH_4 production by the terrestrial biosphere (*42*), such that warmer, wetter climates led to enhanced biospheric CH_4 production and higher atmospheric CH_4 concentrations. Except for a minimum in CH_4 concentrations during the Y-D, the CH_4 increase at the end of the glacial period is roughly in phase with changes in Antarctic temperature, the atmospheric P_{CO_2} increase, and changes in sea level. This result is rather intriguing because the CO_2 response must have originated from the ocean (*43*) whereas the CH_4 signal is of terrestrial origin (*44*).

Increased atmospheric CH_4 concentrations and especially increased atmospheric CO_2 concentrations during the last glacial termination enhanced the greenhouse effect. The magnitude of the greenhouse temperature increase during the last termination is thought to be about 50% of the total warming (*45*). The initial P_{CO_2} increase occurred at about the same time (17 ka) as the initial sea level rise that signaled the end of the last glacial period. Regardless of whether the CO_2 increase was caused by, or resulted from, the start of the deglaciation, increasing concentrations of greenhouse gases must have contributed to the melting of continental ice sheets.

The nature of the deglacial CO_2 increase itself puts some general constraints on possible causes of that increase. First, CO_2 rose from a glacial value of 190 to 200 ppmv to about 230 ppmv by the beginning of the Bølling-Allerod warm period (14.7 ka). This increase obviously cannot have been associated with subsequent changes, such as the main part of the global sea level rise (which occurred between about 14.5 and 10 ka), the Bølling-Allerod warming itself, or the permanent shift in $\delta^{13}C$ of Antarctic deep water at 15 ka as recorded in deep-sea core RC11-83 (Fig. 3). This $\delta^{13}C$ shift presumably reflects the presence of a large component of NADW in the Southern Ocean. Second, CO_2 apparently rose monotonically (*46*) [but see (*47*) for an alternate view]. This feature eliminates the possibility that large parts of the atmospheric CO_2 increase were caused by a rapid shift in surface-water P_{CO_2}.

There are two explanations for the slow and continuous nature of the CO_2 rise. First, the oceanic response time could have been fixed at 5000 to 10,000 years by some characteristic of the oceanic CO_2 cycle. One hypothesis satisfying this constraint invokes a decrease in surface water alkalinity that would have accompanied a deglacial increase in the metabolic CO_2 concentration of intermediate waters at the expense of deep waters (*48, 49*). In this scenario, atmospheric CO_2 rises because the alkalinity of the deep ocean must decrease in order to maintain $CaCO_3$ removal in balance with input. The atmospheric response time is governed by the residence time of CO_3^{2-} in the oceans, about 5000 to 10,000 years (*50*). Although this scenario explains the observed slow rate of CO_2 rise, it accounts for only a small fraction of the atmospheric CO_2 increase for two reasons. First, the deglacial CO_2 redistribution in the Pacific was smaller than Boyle initially estimated (*49, 51*). Second, models of $CaCO_3$ diagenesis in sediments imply that this mechanism can account for only a small part of the observed CO_2 increase (*52*).

A second explanation for the continuous nature of the deglacial CO_2 increase is the coral reef hypothesis (*53, 54*), which suggests that shallow-water $CaCO_3$ precipitation resulting from rising sea level was one contributor to increasing atmospheric CO_2 concentrations. This hypothesis suggests that the rate of CO_2 increase should be roughly linked to the rate of sea level rise, readily explaining the duration of the CO_2 rise of about 7000 years. One problem with this mechanism is that about 60% of the CO_2 increase predates meltwater pulse 1a (at about 14.5 ka), whereas 80% of the sea level rise comes after the start of that event. A second problem is that the CO_2 rise preceded the sea level rise during Termination 2 (*55*). If CO_2 rose for the same reasons during both terminations, then other factors must have caused a large part of that increase.

REFERENCES AND NOTES

1. J. Imbrie *et al.*, *Paleoceanography* **7**, 701 (1992).
2. D. Meese *et al.*, *Technical Report No. 94-1*, "Preliminary depth-age scale of the GISP2 ice core" (Cold Regions Research and Engineering Laboratory, Hanover, NH, 1994).
3. R. B. Alley *et al.*, *Nature* **362**, 527 (1993).
4. M. Bender *et al.*, *ibid.* **372**, 663 (1994).
5. T. Sowers *et al.*, *Paleoceanography* **8**, 737 (1993).
6. H. Craig, Y. Horibe, T. Sowers, *Science* **242**, 1675 (1988).
7. J. Schwander, in *The Environmental Record in Glaciers and Ice Sheets*, H. Oeschger and C. C. Langway, Eds. (Wiley, New York, 1989), pp. 53–67.
8. T. A. Sowers, M. L. Bender, D. Raynaud, *J. Geophys. Res.* **94**, 5137 (1989). We have analyzed the isotopic composition of O_2 and N_2 in trapped fossil air samples using a "wet" extraction technique. We correct the $\delta^{18}O$ of trapped O_2 for gravitational fractionation using the measured $\delta^{15}N$ of trapped N_2 in each sample. Our external precision, based on replicate analyses from the same depth interval, is ±0.05 per mil. We have analyzed 85 samples from the 2196-m Byrd core (80°01′S, 119°31′W, 1530 m above sea level), 108 samples from the upper 2250 m of the GISP II core (72°35′N, 38°29′W, 3207 m above sea level), and 55 samples from the upper 1000 m of the Vostok core (78°28′S, 106°48′E, 3490 m above sea level).
9. M. L. Bender, T. A. Sowers, L. Labeyrie, *Global Biogeochem. Cycles* **8**, 363 (1994).
10. T. Sowers, M. Bender, D. Raynaud, Y. S. Korotkevich, *J. Geophys. Res.* **97**, 15 (1992).
11. D. G. Martinson, W. Menke, P. Stoffa, *ibid.* **87**, 4807 (1982). The resulting mapping function has three coefficients and produced a correlation coefficient of 0.95, suggesting that 90% of the total variance is shared between the two $\delta^{18}O_{atm}$ records. This correlation technique provides an accurate age model for Byrd during periods when $\delta^{18}O_{atm}$ varied rapidly. During the past 35,000 years, the best period for using $\delta^{18}O_{atm}$ as a correlation tool is between 8 and 15 ka. During this 8000 year period, $\delta^{18}O_{atm}$ decreased by 1.4 per mil. To construct an ice age versus depth relation for Byrd, we subtract the maximum Δage values from our earlier study (*10*) from the correlated gas age–depth relation.
12. R. B. Alley and I. M. Whillans, *Science* **254**, 959 (1991).
13. J. Jouzel, R. D. Koster, R. J. Suozzo, G. L. Russel, *J. Geophys. Res.* **99**, 25 (1994).
14. J. Jouzel *et al.*, *ibid.* **92**, 14739 (1987).
15. W. Dansgaard, *Tellus* **16**, 436 (1964).
16. C. D. Charles, D. Rind, J. Jouzel, R. D. Koster, R. G. Fairbanks, *Science* **263**, 508 (1994).
17. W. Dansgaard *et al.*, *Nature* **364**, 218 (1993); P. M. Grootes *et al.*, *ibid.* **366**, 552 (1993).
18. J. Jouzel *et al.*, *Quat. Res.* **31**, 135 (1989).
19. L. D. Keigwin, W. B. Curry, S. J. Lehman, S. Johnsen, *Nature* **371**, 323 (1994).
20. S. J. Lehman and L. Keigwin, *ibid.* **356**, 757 (1992).
21. G. Bond *et al.*, *ibid.* **365**, 143 (1993).
22. S. J. Johnsen *et al.*, *ibid.* **359**, 311 (1992).
23. H. Oeschger *et al.*, in *Climate Processes and Climate Sensitivity*, J. E. Hansen and T. Takahashi, Eds. (Geophysical Monograph No. 29, American Geophysical Union, Washington, DC, 1984), pp. 299–306.
24. J. Jouzel *et al.*, in *The Last Deglaciation: Absolute and Radiocarbon Chronologies*, E. Bard and W. S. Broecker, Eds. (Springer-Verlag, New York, 1992), pp. 229–266. The relation between the $^{18}O/^{16}O$ and D/H ratio of precipitation generally follows the meteoric water line where $\delta D_{prec} = 8\,\delta^{18}O_{prec} + d$, where d is defined as the excess deuterium (*58*). The glacial-interglacial changes in $\delta^{18}O_{ice}$ and δD_{ice} at Byrd and Vostok should have a ratio of 1:8 if (i) the magnitudes of the temperature changes over the two sites were similar, (ii) the source of the precipitation did not change markedly during the transition, and (iii) the other factors controlling the isotopic composition of the precipitation remained constant. The observed glacial-interglacial $\delta^{18}O_{ice}/\delta D_{ice}$ change at Byrd and Vostok is 6 per mil/45 per mil (=1/7.5), which is fairly close to the value predicted on the assumption that the glacial-interglacial temperature change over the two sites was similar.
25. J. D. Hays, J. Lozano, N. Shackleton, G. Irving, in *Investigation of Late Quaternary Paleoceanography and Paleoclimatology*, R. M. a. J. D. H. Cline, Ed. (Memoir 145, Geological Society of America, Boulder, CO, 1976), pp. 337–372.
26. J.-J. Pichon *et al.*, *Paleoceanography* **7**, 289 (1992). We have converted all marine and terrestrial records that are based on ^{14}C dating techniques to calendar years using the appropriate reservoir correction and the calibration program CALIB 3.03 (*60*).
27. R. D. Fairbanks, *Nature* **342**, 637 (1989).
28. T. P. Guilderson, R. G. Fairbanks, J. L. Rubenstone, *Science* **263**, 663 (1994).
29. S. C. Porter, in *Americans Before Columbus*, R. C. Carlisle, Ed. (Department of Anthropology, University of Pittsburgh, Pittsburgh, 1988), vol. 12, pp. 27–48.
30. M. Stute and P. Schlosser, in *Climate Change in Continental Isotopic Records*, P. K. Swart, K. C. Lohmann, J. McKenzie, S. Savin, Eds. (Geophysical Monograph 78, American Geophysical Union, Washington, DC, 1993), pp. 89–100.
31. L. D. Keigwin, G. A. Jones, S. J. Lehman, *J. Geophys. Res.* **96**, 16 (1991).
32. E. Bard *et al.*, *Quat. Res.* **31**, 309 (1989).
33. A. Ruddiman and A. McIntyre, *Palaeogeogr. Palaeoclimatol. Palaeoecol.* **35**, 145 (1981).
34. E. Bard *et al.*, *Quat. Res.* **31**, 381 (1989).
35. T. Veum *et al.*, *Nature* **356**, 783 (1992).
36. C. D. Charles and R. G. Fairbanks, *ibid.*, p. 416.
37. J. Jouzel *et al.*, *Clim. Dyn.*, in press.
38. T. Staffelbach, B. Stauffer, A. Sigg, *Tellus B* **43**, 91 (1991).
39. H. Oeschger, B. Stauffer, R. Finkel, C. C. Langway Jr., in *The Carbon Cycle and Atmospheric CO_2: Natural Variations Archean to Present*, E. T. Sundquist and W. Broecker, Eds. (American Geophysical Union, Washington, DC, 1985), vol. 32, pp. 132–142.
40. R. J. Delmas, *Tellus B* **45**, 391 (1993).
41. J. Chappellaz *et al.*, *Nature* **366**, 443 (1993).
42. J. A. Chappellaz, I. Y. Fung, A. M. Thompson, *Tellus B* **45**, 228 (1993).
43. W. S. Broecker, *Geochim. Cosmochim. Acta* **46**, 1689 (1982).

44. M. A. K. Khalil and M. J. Shearer, in *Atmospheric Methane: Sources, Sinks, and Role in Global Change*, M. A. K. Khalil, Ed. (Springer-Verlag, Heidelberg, 1993), vol. 13, pp. 180–198.
45. C. Lorius *et al.*, *Nature* **347**, 139 (1990).
46. A. Neftel, H. Oeschger, T. Staffelbach, B. Stauffer, *ibid.* **331**, 609 (1988).
47. J. W. C. White *et al.*, *ibid.* **367**, 153 (1994).
48. E. A. Boyle and L. Keigwin, *ibid.* **330**, 35 (1987).
49. E. A. Boyle, *J. Geophys. Res.* **93**, 15 (1988).
50. W. S. Broecker and T.-H. Peng, *Global Biogeochem. Cycles* **1**, 15 (1987).
51. E. A. Boyle, *Annu. Rev. Geophys.* **20**, 245 (1992).
52. S. Emerson and D. Archer, *Paleoceanography* **7**, 319 (1992).
53. W. H. Berger and R. S. Keir, in *Climate Processes and Climate Sensitivity*, J. E. Hansen and T. S. Tadahashi, Eds. (American Geophysical Union, Washington, DC, 1984), vol. 29, pp. 351–357.
54. B. N. Opdyke and J. C. G. Walker, *Geology* **20**, 733 (1992).
55. T. Sowers *et al.*, *Paleoceanography* **6**, 679 (1991).
56. S. J. Johnsen, W. Dansgaard, H. B. Clausen, C. C. Langway Jr., *Nature* **235**, 429 (1972).
57. P. M. Grootes *et al.*, *ibid.* **366**, 552 (1993).
58. R. N. Oldale and C. J. O'Hara, *Geology* **8**, 102 (1980).
59. J. M. Barnola, D. Raynaud, Y. S. Korotkevich, C. Lorius, *Nature* **329**, 408 (1987).
60. M. Stuiver and P. J. Reimer, *Radiocarbon* **35**, 215 (1993).
61. We thank G. Bond, L. Keigwin, D. Peteet, S. Lehman, T. Guilderson, J. Jouzel, and P. Grootes for discussions. This project was funded by NSF grants OPP 93-21623 and OPP 91-1796. This report was funded in part by a grant–cooperative agreement from the National Oceanic and Atmospheric Administration (NOAA). The views expressed herein are those of the authors and do not necessarily reflect the views of NOAA or any of its subagencies. Lamont-Doherty Earth Observatory contribution 5368.

1 March 1995; accepted 5 May 1995

Diurnal Changes in the Partial Pressure of Carbon Dioxide in Coral Reef Water

Hajime Kayanne,*† Atsushi Suzuki, Hiroshi Saito

Coral reefs are considered to be a source of atmospheric carbon dioxide because of their high calcium carbonate production and low net primary production. This was tested by direct measurement of diurnal changes in the partial pressure of carbon dioxide (P_{CO_2}) in reef waters during two 3-day periods, one in March 1993 and one in March 1994, on Shiraho reef of the Ryukyu Islands, Japan. Although the P_{CO_2} values in reef waters exhibited large diurnal changes ranging from 160 to 520 microatmospheres, they indicate that the reef flat area is a net sink for atmospheric carbon dioxide. This suggests that the net organic production rate of the reef community exceeded its calcium carbonate production rate during the observation periods.

Photosynthetic organic production and calcium carbonate production occur simultaneously in coral reefs at rates more than 100 times those in the outer ocean (*1*). Photosynthesis acts as a sink of atmospheric CO_2 ($CO_2 + H_2O \rightarrow CH_2O + O_2$), whereas respiration releases the fixed CO_2. Calcium carbonate production, on the other hand, raises P_{CO_2} in seawater ($Ca^{2+} + 2HCO_3^- \rightarrow CaCO_3 + H_2O + CO_2$). It is thought that gross organic production in reefs is high, but net organic production is near zero, because the tropical ocean is typically depleted in nutrients to support net production. Therefore, coral reefs are thought to be a source of CO_2 to the atmosphere (*2*). One model proposes that the glacial-interglacial increase in atmospheric CO_2 levels resulted from the release of CO_2 that accompanies calcium carbonate deposition in reefs (*3*).

Global productions of net organic carbon and calcium carbonate in reefs have been roughly estimated at 20×10^{12} g of C per year (*4*) and 111×10^{12} g of C per year (*5*), respectively, which supports the hypothesis that coral reefs are a net source for atmospheric CO_2 (*2*). However, knowledge of the actual P_{CO_2} changes that accompany reef productions has been uncertain and requires direct measurement of P_{CO_2} changes in reef water (*6*).

We have monitored the change in P_{CO_2} of reef water over Shiraho coral reef on Ishigaki Island in the Ryukyus of Japan (Fig. 1A). Our measurements were made with a compact seawater P_{CO_2} measurement system with a nondispersive infrared gas analyzer (NDIR) and a membrane tube (*7*). The device is most effectively used in a shallow reef area, which is inaccessible to a large research vessel. We made measurements continuously for two three-day periods, from 9 to 12 March 1993 (Fig. 2A) and from 13 to 17 March 1994 (Fig. 2B). In addition to reef water P_{CO_2}, we measured the partial pressure of CO_2 in the atmosphere (p_{CO_2}), light intensity, current direction and speed, and water depth. P_{CO_2} values outside the reef were measured twice: at 12:00 Japan time on 14 March 1994 and at 0:00 Japan time on 16 March 1994.

Shiraho is a typical fringing reef with a reef flat 850 m wide from the shore to the reef edge. This reef is known for its flourishing corals (Fig. 1B) (*8*). The seaward rise (reef crest) is exposed during low tides and separates water on the reef flat from the outer ocean. This situation is ideal for conducting a natural closed-field experiment. During these stagnant periods, the calcium

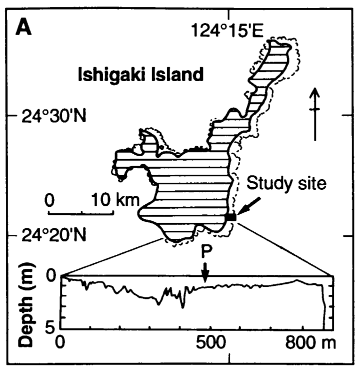

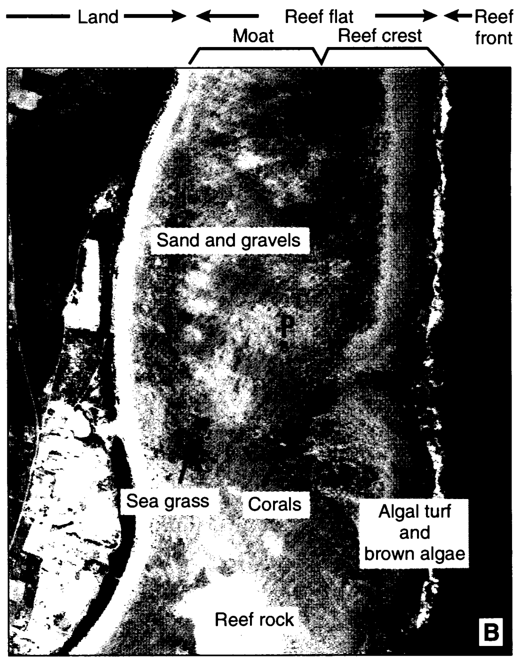

Fig. 1. (**A**) Location of the study site and a transect across the reef flat perpendicular to the shoreline, and (**B**) an aerial photo which shows the monitoring point (P), landforms, and benthic communities. The aerial photo was taken by the Geographical Survey Institute. Reef landforms and communities can be identified by their colors: seagrass in black, sand and gravel in light blue, corals in brown, and algal turf and brown algae in light brown. White color to the south of Shiraho reef shows reef rock covered with sand. The outer reef crest and reef rock are exposed at low tide.

H. Kayanne and A. Suzuki, Marine Geology Department, Geological Survey of Japan, Tsukuba 305, Japan.
H. Saito, Thermophysical Metrology Department, National Research Laboratory of Metrology, Tsukuba 305, Japan.

*To whom correspondence should be addressed.
†Present address: Department of Geography, University of Tokyo, Hongo, Tokyo 113, Japan.